

Numerical Study by Imposing the Finite Difference Method for Unsteady Casson Fluid Flow with Heat Flux

Ali H. Tedjani

Department of Mathematics and Statistics, College of Science, Imam Mohammad Ibn Saud Islamic University (IMSIU), Riyadh, Saudi Arabia

Email: Ahtedjani@imamu.edu.sa

How to cite this paper: Tedjani, A.H. (2023) Numerical Study by Imposing the Finite Difference Method for Unsteady Casson Fluid Flow with Heat Flux. *Journal of Applied Mathematics and Physics*, 11, 3826-3839.

<https://doi.org/10.4236/jamp.2023.1112242>

Received: October 31, 2023

Accepted: December 17, 2023

Published: December 20, 2023

Copyright © 2023 by author(s) and Scientific Research Publishing Inc.

This work is licensed under the Creative Commons Attribution International License (CC BY 4.0).

<http://creativecommons.org/licenses/by/4.0/>



Open Access

Abstract

This article presents an investigation into the flow and heat transfer characteristics of an impermeable stretching sheet subjected to Magnetohydrodynamic Casson fluid. The study considers the influence of slip velocity, thermal radiation conditions, and heat flux. The investigation is conducted employing a robust numerical method that accounts for the impact of thermal radiation. This category of fluid is apt for characterizing the movement of blood within an industrial artery, where the flow can be regulated by a material designed to manage it. The resolution of the ensuing system of ordinary differential equations (ODEs), representing the described problem, is accomplished through the application of the finite difference method. The examination of flow and heat transfer characteristics, including aspects such as unsteadiness, radiation parameter, slip velocity, Casson parameter, and Prandtl number, is explored and visually presented through tables and graphs to illustrate their impact. On the stretching sheet, calculations, and descriptions of the local skin-friction coefficient and the local Nusselt number are conducted. In conclusion, the findings indicate that the proposed method serves as a straightforward and efficient tool for exploring the solutions of fluid models of this kind.

Keywords

Casson Model, Unsteady Stretching Sheet, Variable Heat Flux, MHD, Slip Impacts, Thermal Radiation, Finite Difference Method

1. Introduction

Comprehending the flow of fluid over a stretching sheet is crucial across scientific and engineering realms. This phenomenon plays a fundamental role in ex-

plaining fluid motion dynamics, especially in scenarios involving the stretching or deformation of material surfaces. These situations are prevalent in industries, biomedical applications, and environmental settings. The investigation into fluid flow over a stretching sheet offers valuable insights into the intricate relationships among forces, velocities, and temperature distributions. This contributes significantly to understanding heat transfer mechanisms and optimizing various processes. Ever since Crane [1] analytically presented the solution to the steady flow problem involving a Newtonian fluid propelled by a stretched flat sheet moving within its plane at a velocity that varies linearly with distance from a fixed point, there has been a growing research interest in the flow and heat transfer arising from an unsteady stretching sheet. This heightened interest is attributed to the multitude of practical applications in various sectors of manufacturing processes and technology. In [2], Gupta expanded upon the problem presented by [1] by incorporating a porous sheet, yielding a closed-form solution. Additionally, Grubka and Bobba [3] delved into the thermal field and introduced a solution for the energy equation using Kummer's functions. Numerous other studies have been conducted in the same area of investigation, as documented in [4].

Non-Newtonian fluids are characterized by nonlinear connections between shear stress and strain rate, introducing a notably complex and intricate nature to this type of fluid. Their utilization extends to diverse applications in manufacturing and technology, such as the separation of crude oil from petroleum products. The distinctive rheological behavior of these fluids poses challenges and requires tailored approaches in various industrial processes and technical contexts. Among the various types of non-Newtonian fluids, the Casson fluid class stands out as the most widely recognized, attributed to its widespread use in numerous industrial applications. The thermal transport characteristics of Casson fluids are notably efficient when compared to their Newtonian counterparts. Several additional studies related to the Casson fluid model can be found in ([5] [6] [7]).

Ordinary and partial differential equations have been the focus of extensive investigations due to their recurrent presence in diverse fields such as fluid mechanics, viscoelasticity, biology, physics, and engineering. The solutions to ordinary differential equations (ODEs) with physical relevance have garnered considerable attention, as highlighted in [8]. To quantitatively address the physical problem governed by nonlinear ODEs, the finite difference method was employed as an effective numerical approach. This method aids in obtaining solutions that are crucial for understanding and modeling the behavior of systems across various scientific and engineering domains.

In this article, we demonstrate the use of the implicit finite difference method (FDM) as a numerical method to address the study's main problem. Recent research in this area has begun to significantly include the FDM. Numerous research [9] [10] [11] have shown that this method is a reliable instrument for handling a wide range of issue kinds. The original issue is changed into a nonli-

near system of algebraic equations using this method. The Newton iteration approach will be used to solve the resulting system of nonlinear algebraic equations. The capacity of the FDM to solve problems that occur in calculations with other numerical methods, such as the finite element approach [12], has been noted by numerous scholars [13] [14]. This technique has been utilized to solve various problems [15] [16] [17].

However, the primary objective of this study is to explore the numerical solution for the flow of Casson fluid over a continuously stretching sheet under unsteady conditions, taking into account thermal radiation, a magnetic field, and variable heat flux, all while incorporating slip effect boundary conditions. This research employs the implicit finite difference method to address these complex interactions. The novelty and significance of this investigation lie in its pioneering use of the proposed numerical method to computationally solve the formulated model, marking the first instance of such an approach in this particular context.

2. Methodology

In this segment, we examine the dynamic behavior of two-dimensional unsteady laminar flow and heat transfer involving a non-Newtonian Casson fluid over a stretching sheet that is in motion. The equation describing the rheological state of an incompressible and isotropic fluid flow involving a non-Newtonian Casson fluid has been articulated and thoroughly discussed in prior works, particularly in references [18] [19]. The analysis includes considerations for thermal radiation and variable heat flux based on the thermal radiation. Additionally, we assume a coordinate system where the x -axis aligns with the plane of the sheet, and the y -axis is perpendicular to the plane. We posit that the stretching sheet begins its motion from a stationary position, with the velocity $U(x,t) = \frac{cx}{1-\alpha t}$. Here, c and α are positive constants with units of reciprocal time. In this context, c specifically denotes the initial stretching rate. Similarly, we assume that the surface heat flux $Q(x,t)$ on the stretching sheet exhibits variation based on the power of the distance x from the slit and the power of the time factor, as previously introduced in the reference [20] as follows:

$$Q(x,t) = T_0 (1-\alpha t)^{-m-\frac{1}{2}} dx^r = -\kappa \frac{\partial T}{\partial y}. \quad (1)$$

In this context, T_0 represents the reference temperature, T signifies the temperature of the fluid, κ stands for the thermal conductivity of the Casson fluid, and d is a constant. The variables r and m serve as indices for space and time, respectively. Furthermore, it is posited that the Casson fluid undergoes the influence of two significant and relevant phenomena: magnetic forces and thermal radiation [21]. These factors play a pivotal role in governing the heat transfer process within the fluid flow. Moreover, the simplification applied to express thermal radiation in a linear form is expounded in detail in reference [21]. The time-dependent velocity and temperature fields that govern the flow described

in this manner are outlined as follows, as referenced in [22]:

$$\frac{\partial u}{\partial x} + \frac{\partial v}{\partial y} = 0, \quad (2)$$

$$u \frac{\partial u}{\partial x} + v \frac{\partial u}{\partial y} + \frac{\partial u}{\partial t} = \frac{1}{\rho} \frac{\partial}{\partial y} \left(\mu (1 + \gamma^{-1}) \frac{\partial u}{\partial y} \right) - \frac{\sigma B_0^2}{\rho} u, \quad (3)$$

$$u \frac{\partial T}{\partial x} + v \frac{\partial T}{\partial y} + \frac{\partial T}{\partial t} = \frac{\kappa}{\rho c_p} \left(1 + \frac{16\sigma^* T_\infty^3}{3k^* \kappa} \right) \frac{\partial^2 T}{\partial y^2}, \quad (4)$$

here, the components of velocity along the x and y directions are denoted by u and v respectively. In this context, μ represents the viscosity of the fluid, ρ signifies the density of the fluid, σ stands for the electric conductivity, B_0 represents the strength of the magnetic field, γ is indicative of the Casson parameter, and c_p corresponds to the specific heat at constant pressure. The suitable boundary conditions for the current problem are as follows [20] [22]:

$$u = \frac{cx}{1 - \alpha t} + \lambda_1 \left(1 + \frac{1}{\gamma} \right) \frac{\partial u}{\partial y}, \quad v = 0, \quad -\kappa \frac{\partial T}{\partial y} = Q(x, t) \quad \text{at } y = 0, \quad (5)$$

$$T \rightarrow T_\infty, \quad u \rightarrow 0, \quad \text{as } y \rightarrow \infty, \quad (6)$$

where λ_1 denotes the velocity slip factor, a parameter that dynamically varies over time. The simplification of the mathematical analysis of the problem is achieved by introducing the subsequent dimensionless coordinates [20]:

$$u = \frac{cx}{1 - \alpha t} f'(\eta), \quad \eta = \left(\frac{c}{\nu} \right)^{\frac{1}{2}} (1 - \alpha t)^{-\frac{1}{2}} y, \quad v = -\frac{\sqrt{c\nu}}{(1 - \alpha t)^{\frac{1}{2}}} f(\eta), \quad (7)$$

$$T = T_\infty + T_0 \left(\frac{dx'}{\kappa \sqrt{c/\nu}} \right) (1 - \alpha t)^{-m} \theta(\eta), \quad (8)$$

In this context, $f(\eta)$ represents the dimensionless stream function, and $\theta(\eta)$ denotes the dimensionless temperature. Moreover, by the final equation, the temperature of the sheet, denoted as T_w , can be expressed as follows $T_w = T_\infty + T_0 \left(\frac{dx'}{\kappa \sqrt{c/\nu}} \right) (1 - \alpha t)^{-m} \theta(0)$. By employing Equations (7)-(8), the mathematical problem delineated in Equations (2)-(4) is subsequently converted into a system of ordinary differential equations along with their corresponding boundary conditions:

$$(1 + \gamma^{-1}) f''' - \Lambda \left(f' + \frac{\eta}{2} f'' \right) - f'^2 + ff'' - Mf' = 0, \quad (9)$$

$$\frac{1}{Pr} (1 + R) \theta'' + f \theta' - \Lambda \left(m\theta + \frac{\eta}{2} \theta' \right) - rf' \theta = 0, \quad (10)$$

$$f = 0, \quad \theta' = -\frac{1}{1 + R}, \quad f' = 1 + \lambda(1 + \gamma^{-1}) f'', \quad \text{at } \eta = 0, \quad (11)$$

$$f' \rightarrow 0, \quad \theta \rightarrow 0 \quad \text{as } \eta \rightarrow \infty. \quad (12)$$

Here, the prime symbol signifies differentiation concerning η , and the para-

parameters are defined as follows: Λ represents the unsteadiness parameter, given by $\Lambda = \frac{\alpha}{c}$; R is the radiation parameter, expressed as $R = \frac{16\sigma^* T_\infty^3}{3k^* \kappa}$; M denotes the magnetic parameter, calculated as $M = \frac{\sigma B_0^2}{c\rho}$; and Pr stands for the Prandtl number, defined as $Pr = \frac{\rho \nu c_p}{\kappa}$. In the realm of engineering and practical applications, our focus is directed toward exploring crucial physical attributes related to flow behavior and heat transfer characteristics. This exploration involves the analysis of non-dimensional quantities, specifically the local skin friction coefficient (Cf_x) or fractional drag coefficient, and the local Nusselt number (Nu_x). The definitions of these non-dimensional parameters are articulated as follows:

$$Cf_x = -2Re_x^{-1} \left(1 + \frac{1}{\gamma}\right) f''(0), \quad Nu_x = \frac{Re_x^{\frac{1}{2}}}{\theta(0)},$$

where $Re_x = \frac{Ux}{\nu}$ is the local Reynolds number.

3. Solution Procedure Using FDM

Our aim in this section is to use the FDM to solve Equations (9)-(10) with the boundary conditions (11)-(12). This method has been tested for accuracy and efficiency in solving different problems. We use the transformation $f'(\eta) = \phi(\eta)$ to rewrite the system of Equations (9)-(12) in the following form:

$$f' - \phi = 0, \quad (13)$$

$$(1 + \gamma^{-1})\phi'' - \Lambda(\phi + 0.5\eta\phi') - \phi^2 + f\phi' - M\phi = 0, \quad (14)$$

$$(1 + R)\theta'' + Pr f\theta' - Pr\Lambda(m\theta + 0.5\eta\theta') - rPr\phi\theta = 0, \quad (15)$$

$$f(0) = 0, \quad \theta'(0) = -(1 + R)^{-1}, \quad \phi(0) = 1 + \lambda(1 + \gamma^{-1})\phi'(0), \quad (16)$$

$$\phi(\eta_\infty) = 0, \quad \theta(\eta_\infty) = 0. \quad (17)$$

In finite difference methods the space of solution's domain is discretized. We use the notations $\Delta\eta = \hbar > 0$ to be the grid size in η -direction, $\Delta\eta = \eta_\infty/N$, with $\eta_k = k\hbar$ for $k = 0, 1, \dots, N$. Define $f_k = f(\eta_k)$, $\phi_k = \phi(\eta_k)$ and $\theta_k = \theta(\eta_k)$.

Let F_k, Φ_k , and Θ_k denote the numerical values of f, ϕ , and θ at the k^{th} node, respectively. We take

$$f'|_k \approx \frac{f_{k+1} - f_{k-1}}{2\hbar}, \quad \phi'|_k \approx \frac{\phi_{k+1} - \phi_{k-1}}{2\hbar}, \quad \theta'|_k \approx \frac{\theta_{k+1} - \theta_{k-1}}{2\hbar}, \quad (18)$$

$$\phi''|_k \approx \frac{\phi_{k+1} - 2\phi_k + \phi_{k-1}}{\hbar^2}, \quad \theta''|_k \approx \frac{\theta_{k+1} - 2\theta_k + \theta_{k-1}}{\hbar^2}. \quad (19)$$

The main step is that the system of ODEs (13)-(17) is discretized in space by using FDM. To do this we substitute from (18)-(19) into (13)-(17) and neglect

the truncation errors, the resulting algebraic equations take the form:

$$F_{k+1} - F_{k-1} - 2\hbar\Phi_k = 0, \quad k = 0, 1, \dots, N, \quad (20)$$

$$\begin{aligned} (1 + \gamma^{-1})(\Phi_{k+1} - 2\Phi_k + \Phi_{k-1}) - \Lambda(\hbar^2\Phi_k + 0.25\hbar\eta_k(\Phi_{k+1} - \Phi_{k-1})) \\ - \hbar^2\Phi_k^2 + 0.5\hbar F_k(\Phi_{k+1} - \Phi_{k-1}) - \hbar^2 M \Phi_k = 0, \end{aligned} \quad (21)$$

$$\begin{aligned} (1 + R)(\Theta_{k+1} - 2\Theta_k + \Theta_{k-1}) + 0.5\hbar Pr F_k(\Phi_{k+1} - \Phi_{k-1}) \\ - \Lambda Pr(m\hbar^2\Theta_k + 0.25\hbar\eta_k(\Theta_{k+1} - \Theta_{k-1})) - \hbar^2 r Pr \Phi_k \Theta_k = 0. \end{aligned} \quad (22)$$

Also, the boundary conditions are:

$$\begin{aligned} F_0 = 0, \quad \Theta_1 - \Theta_0 + 2\hbar(1 + R)^{-1}, \quad \Phi_N = \Theta_N = 0, \\ \Phi_0 = 1 + 0.5\hbar^{-1}\lambda(1 + \gamma^{-1})(\Phi_1 - \Phi_0). \end{aligned} \quad (23)$$

The system of Equations (20)-(23) is a non-linear system of algebraic equations in the variables F_k, Φ_k , and Θ_k , ($k = 0, 1, \dots, N$). In our calculation using the Mathematica Package, and Newton iteration method with suitable initial solutions to solve numerically this system.

4. Results and Discussion

The preceding examination delved into the impact of variable heat flux on the flow characteristics of a magnetohydrodynamics (MHD) non-Newtonian Casson fluid with slip conditions over an unsteady stretching sheet. This investigation also considered the concurrent influence of thermal radiation on heat transfer phenomena within the system. In this particular segment, our focus will shift towards a comprehensive exploration of the characteristics exhibited by the physical parameters that play a pivotal role in shaping the dynamics of the formulated model. These parameters include the Casson parameter denoted as γ , the magnetic parameter represented by M , the unsteady parameter identified as Λ , the time indices parameter denoted as m , the velocity slip parameter indicated by λ , the space indices parameter represented by r , and lastly, the Prandtl number denoted as Pr . **Figure 1(a)** and **Figure 1(b)** scrutinize the impact of the magnetic number denoted as M on the profiles of velocity and temperature, respectively. **Figure 1(a)** illustrates that the velocity experiences a decline as a function of the magnetic number M while **Figure 1(b)** depicts an increasing trend with the same parameter M . This behavior can be attributed to the physical phenomenon associated with magnetic fields, which generate the Lorentz force. The Lorentz force acts in opposition to the flow, leading to a reduction in fluid velocity.

Figure 2(a) is constructed to elaborate on the dimensionless velocity distribution within the boundary layer across various values of the unsteadiness parameter Λ . The observation drawn from this figure indicates that an augmentation in the unsteadiness parameter results in a decrease in the velocity distribution within the boundary layer. Conversely, as a consequence of the heat flux prevailing along the sheet, it is observed that the temperature distribution within

the boundary layer, as well as the wall temperature denoted as $\theta(0)$, demonstrates an increase with a corresponding rise in the aforementioned parameter, as depicted in **Figure 2(b)**. In terms of physical interpretation, this behavior emphasizes a fundamental aspect: the cooling rate is significantly accelerated for smaller values of the unsteadiness parameter. Conversely, larger values of the unsteadiness parameter may necessitate a more prolonged duration for the cooling process.

Figure 3(a) and **Figure 3(b)** have been meticulously illustrated to provide a clearer understanding of how the velocity slip parameter, denoted as λ affects both velocity and temperature profiles. The purpose of these figures is to elucidate and shed light on the intricate relationship between the parameter λ and the respective profiles of velocity and temperature. By examining **Figure 3(a)**, it can

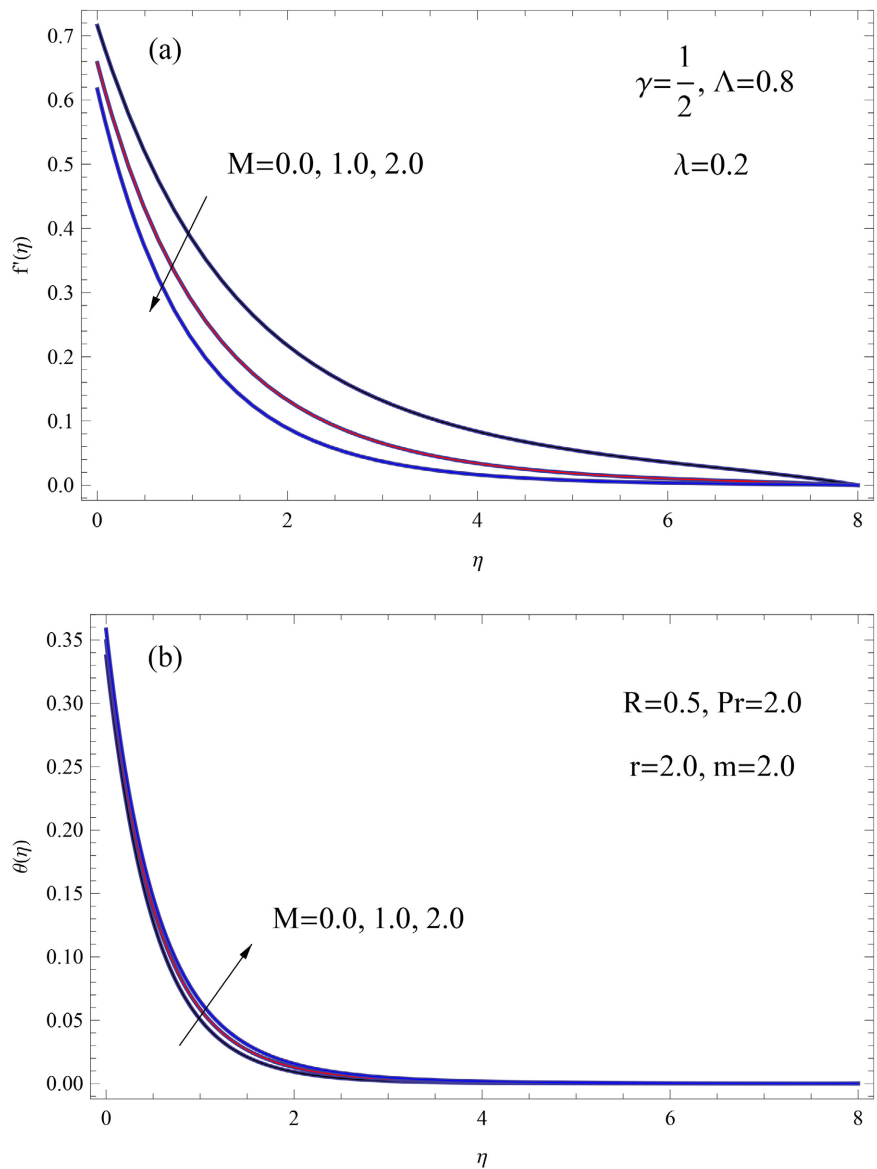


Figure 1. (a) Velocity distribution for M , (b) Temperature distribution for M .

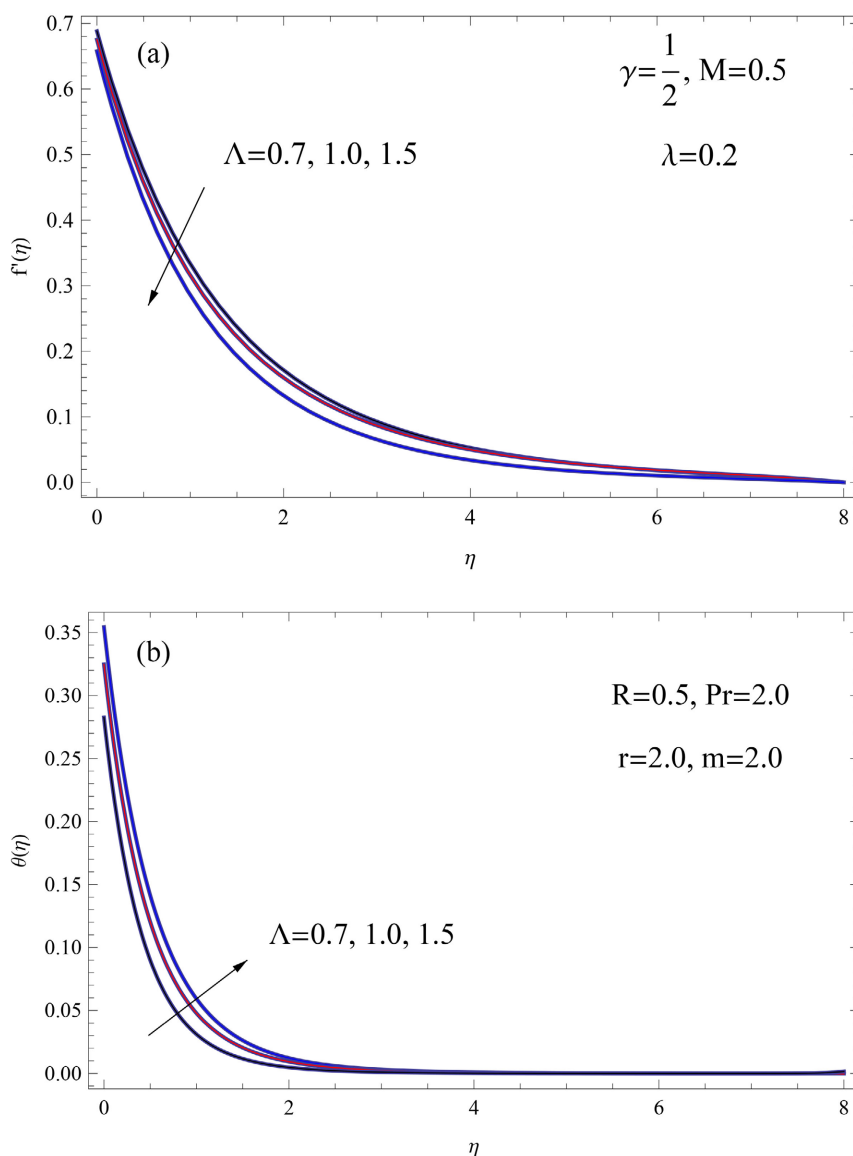


Figure 2. (a) Velocity distribution for Λ , (b) Temperature distribution for Λ .

be noted that as the slip velocity parameter increases, there is a noticeable reduction in both the velocity distribution within the boundary layer and the thickness of the boundary layer. Physically, the introduction of slip conditions implies that the fluid exhibiting slip reduces the surface skin friction values between the fluid and the stretching sheet. Consequently, an increase in the slip velocity parameter results in a decrease in the flow velocity within the boundary layer region. **Figure 3(b)** depicts the dimensionless temperature distribution within the boundary layer region corresponding to the slip velocity parameter. An increase in the velocity slip parameter, as observed in the figure, is associated with higher temperatures at the wall ($\theta(0)$) and an enhanced distribution of fluid temperature within the thermal boundary layer. These observations imply that changes in the velocity slip parameter significantly influence not just the temperature at the wall but also the broader thermal characteristics within the boundary layer.

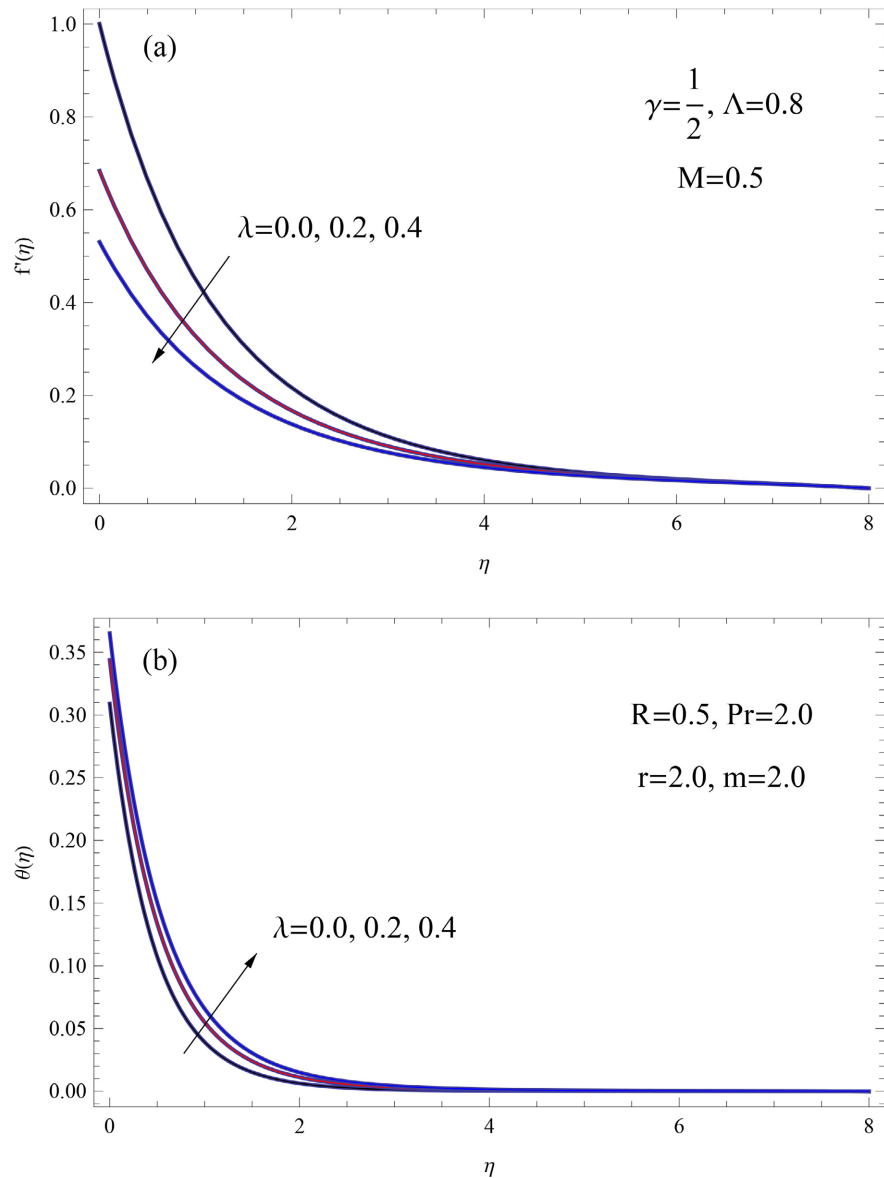


Figure 3. (a) Velocity distribution for λ , (b) Temperature distribution for λ .

In the subsequent illustration presented in **Figure 4(a)**, the velocity distribution is displayed as a function of the similarity variable η across different values of the Casson parameter γ . This graphical representation aims to provide a visual depiction of how the velocity varies concerning the similarity variable for various settings of the Casson parameter γ . The depicted Figure illustrates that augmenting the Casson parameter results in an elevation of the velocity distribution along the sheet, whereas the opposite trend is observed away from the sheet. Furthermore, an increase in the Casson parameter is associated with a reduction in the thickness of the boundary layer. **Figure 4(b)** displays the impact of the radiation parameter on the temperature profile. This graphical representation is designed to elucidate how variations in the radiation parameter influence the distribution of temperature within the system. It is clear from the observations

that an escalation in the radiation parameter has the effect of amplifying the temperature distribution along the boundary layer while concurrently causing a reduction in the temperature at the surface, denoted as $\theta(0)$.

Illustrated in **Figure 5** is the influence of the Prandtl number, denoted as Pr , on the temperature profiles above the sheet. Upon careful examination of this figure, it becomes apparent that a reduction in the Prandtl number contributes to an augmentation in the thickness of the thermal boundary layer, the distribution of temperature, and the temperature at the wall, represented by $\theta(0)$. This phenomenon can be attributed to the physical observation that higher values of the Prandtl number are indicative of weaker thermal diffusivity.

Table 1 reveal the effect of different values of physical governing parameters of the magnetic parameter M , the Casson parameter β , the unsteady parameter S ,

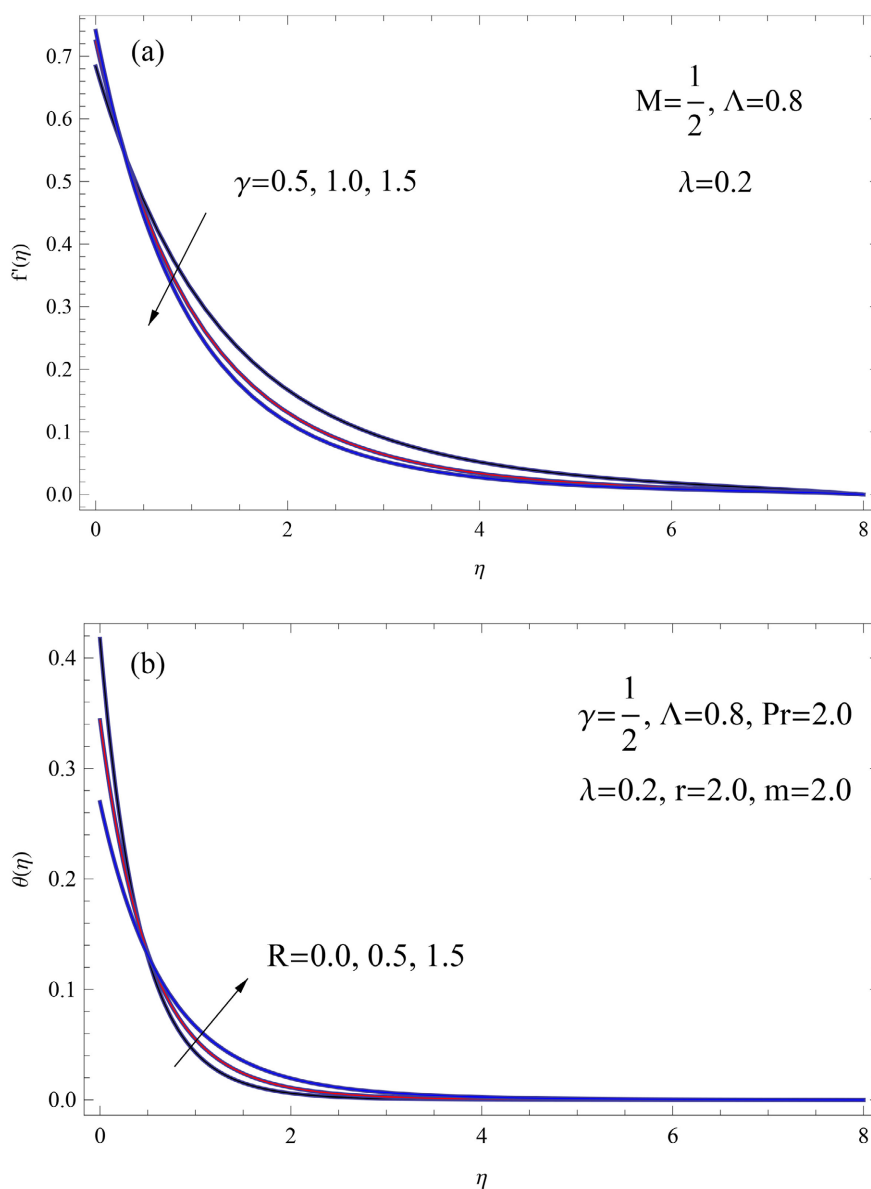


Figure 4. (a) Velocity distribution for γ , (b) Temperature distribution for R .

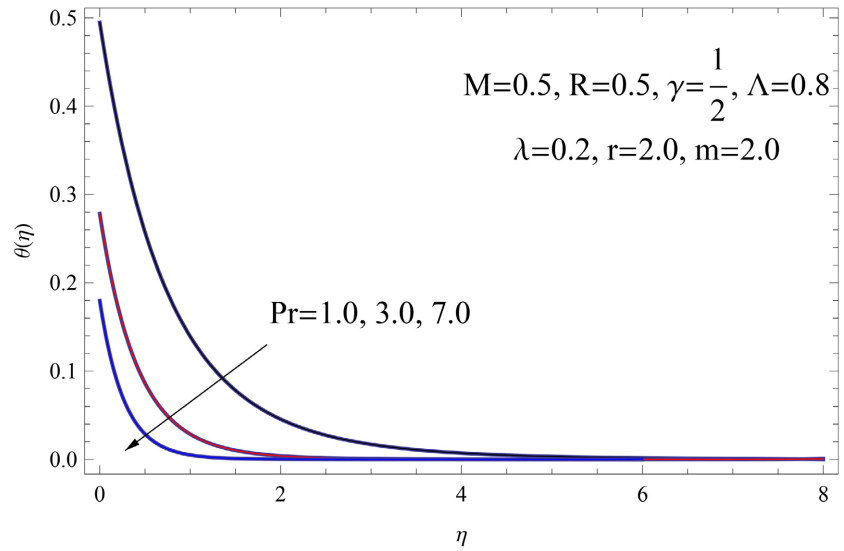


Figure 5. Temperature distribution for Pr .

Table 1. Variation of $-\left(1+\frac{1}{\gamma}\right)f''(0)$ and $\frac{1}{\theta(0)}$ for various values of $M, \Lambda, \lambda, \gamma, R$ and Pr .

M	Λ	λ	γ	R	Pr	$-\left(1+\frac{1}{\gamma}\right)f''(0)$	$\frac{1}{\theta(0)}$
0.0	0.8	0.2	0.5	0.5	2.0	1.42101	2.96573
1.0	0.8	0.2	0.5	0.5	2.0	1.71145	2.86408
2.0	0.8	0.2	0.5	0.5	2.0	1.91604	2.79193
0.5	0.7	0.2	0.5	0.5	2.0	1.55898	2.82161
0.5	1.0	0.2	0.5	0.5	2.0	1.62378	3.07891
0.5	1.5	0.2	0.5	0.5	2.0	1.88450	3.67287
0.5	0.8	0.0	0.5	0.5	2.0	2.50577	3.23579
0.5	0.8	0.2	0.5	0.5	2.0	1.58118	2.90983
0.5	0.8	0.4	0.5	0.5	2.0	1.17388	2.73923
0.5	0.8	0.2	0.5	0.5	2.0	1.58118	2.90983
0.5	0.8	0.2	1.0	0.5	2.0	1.38137	2.92291
0.5	0.8	0.2	1.5	0.5	2.0	1.29648	2.92520
0.5	0.8	0.2	0.5	0.0	2.0	1.58118	2.39589
0.5	0.8	0.2	0.5	0.5	2.0	1.58118	2.90983
0.5	0.8	0.2	0.5	1.5	2.0	1.58118	3.70911
0.5	0.8	0.2	0.5	0.0	2.0	1.58118	2.02109
0.5	0.8	0.2	0.5	0.5	2.0	1.58118	3.59383
0.5	0.8	0.2	0.5	1.5	2.0	1.58118	5.56367

time indices parameter m , space indices parameter r , the heat generation parameter, the Prandtl number Pr , the velocity slip parameter λ and the Eckert

number Ec as these are required for the evaluation of the local skin-friction coefficient $\frac{1}{2}Cf_x Re_x^{\frac{1}{2}}$ and the local Nusselt number $Nu_x Re_x^{-\frac{1}{2}}$. It is seen that the increase in the unsteady parameter causes an increase in both the skin friction coefficient and local Nusselt number. Also, the local skin-friction coefficient decreases by increasing the Casson parameter, whereas the local Nusselt number increases with the increasing values it. With the increase in the slip velocity parameter λ both the local skin-friction coefficient and the local Nusselt number decrease. Moreover, it is noticed that increases in the values of the Eckert number and the heat generation parameter lead to a decrease in the local Nusselt number. On the other hand, an increase in the Prandtl number causes an increase in the local Nusselt number. This is because fluid with a higher value of Prandtl number possesses a large heat capacity, and hence intensifies the heat transfer. Finally, the local Nusselt number increases as the space indices parameter, the heat absorption parameter, and the time indices parameter increases.

5. Conclusion

This research systematically investigates the influence of slip effects, thermal radiation, variable heat flux, and a magnetic field on the boundary layer flow and heat transfer of a Casson fluid over an unsteady stretching sheet. By employing appropriate dimensionless transformations, the governing partial differential equations are transformed into ordinary differential equations. These equations are then solved numerically using the finite difference method. The overarching goal of this comprehensive study is to understand how the interplay of these diverse factors collectively shapes the flow dynamics and heat transfer characteristics in the scenario of a Casson fluid interacting with an unsteady stretching sheet. The impact of increasing either the unsteadiness parameter or the Prandtl number on the local Nusselt number has been documented. Additionally, it was observed that an elevation in the slip velocity parameter results in a decrease in both the local skin friction coefficient and the local Nusselt number. Conversely, as the radiation parameter increases, the local Nusselt number decreases, whereas an opposite trend is noted for the Casson parameter.

Acknowledgements

Sincere thanks to the members of JAMP for their professional performance, and special thanks to managing editor for a rare attitude of high quality.

Conflicts of Interest

The authors declare no conflicts of interest regarding the publication of this paper.

References

- [1] Crane, L.J. (1970) Flow past a Stretching Plate. *Zeitschrift für angewandte Mathe-*

- matik und Physik*, **21**, 645-647. <https://doi.org/10.1007/BF01587695>
- [2] Gupta, P.S. and Gupta, A.S. (1977) Heat and Mass Transfer on a Stretching Sheet with Suction or Blowing. *Canadian Journal of Chemical Engineering*, **55**, 744-746. <https://doi.org/10.1002/cjce.5450550619>
- [3] Grubka, L.J. and Bobba, K.M. (1985) Heat Transfer Characteristics of a Continuous Stretching Surface with Variable Temperature. *ASME Journal of Heat Transfer*, **107**, 248-250. <https://doi.org/10.1115/1.3247387>
- [4] Chen, C.K. and Char, M. (1988) Heat Transfer on a Continuous, Stretching Surface with Suction or Blowing. *Journal of Mathematical Analysis and Applications*, **35**, 568-580. [https://doi.org/10.1016/0022-247X\(88\)90172-2](https://doi.org/10.1016/0022-247X(88)90172-2)
- [5] Ghadikolaei, S.S., Hosseinzadeh, K. and Jafari, G.B. (2018) Nonlinear Thermal Radiation Effect on Magneto Casson Nanofluid Flow with Joule Heating Effect over an Inclined Porous Stretching Sheet. *Case Studies in Thermal Engineering*, **12**, 176-187. <https://doi.org/10.1016/j.csite.2018.04.009>
- [6] Lund, L.A., Omar, Z., Khan, I., Baleanu, D. and Nisar, K.S. (2020) Dual Similarity Solutions of MHD Stagnation Point Flow of Casson Fluid with Effect of Thermal Radiation and Viscous Dissipation: Stability Analysis. *Scientific Reports*, **10**, Article No. 15405. <https://doi.org/10.1038/s41598-020-72266-2>
- [7] Sarkar, S. and Endalew, M.F. (2019) Effects of Melting Process on the Hydromagnetic Wedge Flow of a Casson Nanofluid in a Porous Medium. *Boundary Value Problem*, **2019**, Article No. 43. <https://doi.org/10.1186/s13661-019-1157-5>
- [8] Yaslan, H.Ç. (2017) Numerical Solution of Fractional Riccati Differential Equation via Shifted Chebyshev Polynomials of the Third Kind. *Journal of Engineering Technology and Applied Sciences*, **2**, 1-11.
- [9] Butcher, J.C. (2003) Numerical Methods for Ordinary Differential Equations. John Wiley & Sons, Hoboken. <https://doi.org/10.1002/0470868279>
- [10] Khader, M.M. and Adel, M. (2016) Numerical Solutions of Fractional Wave Equations Using an Efficient Class of FDM Based on Hermite Formula. *Advances in Difference Equations*, **2016**, Article No. 34. <https://doi.org/10.1186/s13662-015-0731-0>
- [11] Khader, M.M. (2019) Fourth-Order Predictor-Corrector FDM for the Effect of Viscous Dissipation and Joule Heating on the Newtonian Fluid Flow. *Computers and Fluids*, **182**, 9-14. <https://doi.org/10.1016/j.compfluid.2019.02.011>
- [12] Khader, M.M. and Sharma, R.P. (2021) Evaluating the Unsteady MHD Micropolar Fluid Flow past Stretching/Shirking Sheet with Heat Source and Thermal Radiation: Implementing Fourth Order Predictor-Corrector FDM. *Mathematics and Computers in Simulation*, **181**, 333-350. <https://doi.org/10.1016/j.matcom.2020.09.014>
- [13] Khader, M.M. (2011) On the Numerical Solutions for the Fractional Diffusion Equation. *Communications in Nonlinear Science and Numerical Simulation*, **16**, 2535-2542. <https://doi.org/10.1016/j.cnsns.2010.09.007>
- [14] Sweilam, N.H., Khader, M.M. and Nagy, A.M. (2011) Numerical Solution of Two-Sided Space Fractional Wave Equation Using FDM. *The Journal of Computational and Applied Mathematics*, **235**, 2832-2841. <https://doi.org/10.1016/j.cam.2010.12.002>
- [15] Khader, M.M., Sweilam, N.H. and Mahdy, A.M.S. (2013) Numerical Study for the Fractional Differential Equations Generated by Optimization Problem Using Chebyshev Collocation Method and FDM. *Applied Mathematics and Information Science*, **7**, 2013-2020. <https://doi.org/10.12785/amis/070541>

-
- [16] Johnston, H. and Liu, J.G. (2002) Finite Difference Schemes for Incompressible Flow Based on Local Pressure Boundary Conditions. *Journal of Computational Physics*, **180**, 120-154. <https://doi.org/10.1006/jcph.2002.7079>
- [17] Zakaria, M., Khader, M.M., Ibrahim, A. and Al-Tayeb, W. (2022) Solving Fractional Generalized Fisher-Kolmogorov-Petrovsky-Piskunov's Equation Using Compact Finite Difference Method Together with Spectral Collocation Algorithms. *Journal of Mathematics*, **2022**, Article ID: 1901131. <https://doi.org/10.1155/2022/1901131>
- [18] Megahed, A.M. (2015) Effect of Slip Velocity on Casson Thin Film Flow and Heat Transfer Due to an Unsteady Stretching Sheet in the Presence of Variable Heat Flux and Viscous Dissipation. *Applied Mathematics and Mechanics*, **36**, 1273-1284. <https://doi.org/10.1007/s10483-015-1983-9>
- [19] Megahed, A.M. (2016) Heat Flux and Variable Thermal Conductivity Effects on Casson Flow and Heat Transfer Due to an Exponentially Stretching Sheet with Viscous Dissipation and Heat Generation. *International Journal of Chemical Reactor Engineering*, **14**, 167-174. <https://doi.org/10.1515/ijcre-2015-0135>
- [20] Megahed, A.M. (2014) Variable Heat Flux Effect on MHD Flow and Heat Transfer over an Unsteady Stretching Sheet in the Presence of Thermal Radiation. *Canadian Journal of Physics*, **92**, 86-91. <https://doi.org/10.1139/cjp-2012-0543>
- [21] Megahed, A.M., et al. (2021) Modeling of MHD Fluid Flow over an Unsteady Stretching Sheet with Thermal Radiation, Variable Fluid Properties and Heat Flux. *Mathematics and Computers in Simulation*, **185**, 583-593. <https://doi.org/10.1016/j.matcom.2021.01.011>
- [22] Mostafa, A.A.M. and Megahed, A.M. (2017) MHD Flow and Heat Transfer Characteristics in a Casson Liquid Film towards an Unsteady Stretching Sheet with Temperature Dependent Thermal Conductivity. *Brazilian Journal of Physics*, **47**, 512-523. <https://doi.org/10.1007/s13538-017-0518-8>